Solvatochromism and linear solvation energy relationship of diol- and proline-functionalized azo dyes using the Kamlet–Taft and Catalán solvent parameter sets†

Katja Hofmann,[a] Katja Schreiter,[a] Andreas Seifert,[a] Tobias Rüffer,[b] Heinrich Lang[b] and Stefan Spange*[a]

Received (in Montpellier, France) 2nd June 2008, Accepted 4th July 2008
First published as an Advance Article on the web 8th September 2008
DOI: 10.1039/b809055f

New donor–acceptor-substituted azo dyes, such as 2-({4-[(*E*)-(2,4-dinitrophenyl)diazenyl]-2-nitrophenyl}amino)propane-1,3-diol, (2*S*)-1-{4-[(*E*)-(2,4-dinitrophenyl)diazenyl]-2-nitrophenyl}-pyrrolidine-2-carboxylic acid and methyl-(2*S*)-1-{4-[(*E*)-(2,4-dinitrophenyl)diazenyl]-2-nitrophenyl}pyrrolidine-2-carboxylate have been obtained in a single step by nucleophilic aromatic substitution of (*E*)-1-(2,4-dinitrophenyl)-2-(4-fluoro-3-nitrophenyl)diazene with 2-aminopropane-1,3-diol, (*S*)-proline and (*S*)-proline methyl ester hydrochloride. The solvatochromism of the diol- and (*S*)-proline-methyl-ester-containing azo dye was studied and analysed using the empirical Kamlet–Taft and Catalán solvent parameter set. The dyes undergo a reversible protonation–deprotonation equilibrium in a concentration range of 5–12 M hydrochloric acid. The UV/Vis absorption spectra show a bathochromic shift with increasing acid strength of the medium.

Introduction

Azo dyes have gained wide interest and found many uses in materials for optical applications and in analysis. Due to their properties, including optical storage capacity,[1] optical switching,[2] holography[1a,3] and non-linear optical properties (NLO),[4] polymers with azo units represent promising candidates for photoactive materials. Donor–acceptor-substituted azobenzenes are a well-known family of organic dyes. Their colors can be changed by selection of the strength of the donor and/or acceptor groups.[5] Such push–pull-substituted compounds can also act as acid–base (*p*H dependent),[6] and solvent-sensitive (solvatochromic)[7] indicators.

Interactions of solvatochromic dyes with pure solvents or solvent mixtures are a combination of many effects.[8] Many intermolecular specific and nonspecific solute–solvent interactions can be described using the concept of linear free energy relationships (LSERs)[8a,b] (general eqn (1a)).

$$(XYZ) = (XYZ)_0 + aA + bB + cC \qquad (1a)$$

Here $(XYZ)_0$ represents the physico-chemical property in a nonpolar medium; *a*, *b* and *c* are solvent–independent coefficients, which reflect the dependence of the physical and chemical properties (*XYZ*) in a particular solvent on various solvent parameters (*A*, *B*, *C*).

The original Kamlet–Taft[9] equation has been verified in the literature many times and is one of the most promising and successful quantitative methods of describing solvent effects with a multiparameter equation. In its simplified form, as in eqn (1b), the effect of the acidity α[9a] (α corresponds to *A*) (hydrogen bond donor capacity), the basicity β[9b] (β corresponds to *B*) (hydrogen bond acceptor capacity) and the dipolarity/polarizability π^*[9c,d] (π^* corresponds to *C*) of a solvent can be expressed using a multiparameter equation. For the determination of the α, β, and π^* values, Kamlet and Taft drew on a large number of medium-dependent chemical processes, among which were a large number of solvatochromic dyes. The disadvantage of the Kamlet–Taft parameter is as follows. It is not based on a defined reference process, but represents the average of several solvent-dependent processes. In spite of these critical aspects, the Kamlet–Taft parameters have been used for the interpretation of physico-chemical processes in many areas during the last three decades.

In the last 10 years Catalán *et al.* have developed four empirical solvent parameter scales.[10] On the basis of α and β, the *SA* (*SA* corresponds to *A*) (solvent acidity)[10b,c] and *SB* (*SB* corresponds to *B*) (solvent basicity)[10d] scales were established. The dipolarity/polarizability is reflected by the parameter *SPP*.[10e,f] comparable with Kamlet–Taft's π^* value. A further parameter, the so-called *SP* parameter[10g] (solvent polarizability) is really new. Up to now empirical polarity scales, such as π^*, have always described the dipolarity and the polarizability of a solvent at the same time. This presupposes that a change in the polarity of the solvent is accompanied by a clear change in the dipole moment of the solvatochromic probe. Abe[11] has

[a] *Department of Polymer Chemistry, Institute of Chemistry, Chemnitz University of Technology, Strasse der Nationen 62, 09111 Chemnitz, Germany. E-mail: stefan.spange@chemie.tu-chemnitz.de; Fax: +49 (0)371-531-21230; Tel: +49 (0)371-531-21239*
[b] *Department of Inorganic Chemistry, Institute of Chemistry, Chemnitz University of Technology, Strasse der Nationen 62, 09111 Chemnitz, Germany*

† Electronic supplementary information (ESI) available: Kamlet–Taft and Catalán parameter set, all results of the multiple linear regression analyses. CCDC reference number 680370. For ESI and crystallographic data in CIF or other electronic format see DOI: 10.1039/b809055f

already proposed that these scales are reaching their limits with low polarity substances. For this reason Catalán *et al.* has now developed an empirical scale which describes only one of these effects, the polarizability.[10g] Thus, *C* from eqn (1a) corresponds to *SPP* (eqn (1c)) and *SP* (eqn (1d)), respectively. The advantage of the Catalán scales lies principally in the fact that they are based on a defined reference process. Because of this, there are certain clear differences between them and the Kamlet–Taft parameters.[12]

In this work we present the new diol- and amino-acid-functionalized azobenzenes **2a–c**, which are synthesized by nucleophilic aromatic substitution of the fluorine-functionalized azo dye (*E*)-1-(2,4-dinitrophenyl)-2-(4-fluoro-3-nitrophenyl)-diazene (**1**).[13] The synthetic aspects, the structural considerations of the structure in the solid state and the hydrogen bonding pattern are discussed as well. Specific functionalization by diol substituents allows binding to boronic acids[14] and fatty acids to detect fluoride and cyanide ions, as well as for the construction of chromophoric lipid layers. N-substituted amino acids can be coupled with other amino acids, dipeptides or oligopeptides.[15] Thus, new types of non-fluorescent dyes are accessible as temporary markers in peptide chemistry.[16] This specific choice of substituent offers the possibility of building up many types of coupled structures. A possible challenging application is the functionalization with these chromophores of, for example, dendrimers either at the focal point or at the periphery. The solvatochromism of these substances could therefore be studied as a function of a particular generation number.

With regard to these potential applications we investigated the solvatochromism of the new diol- and proline functionalized azo dyes **2a** and **2c**. In this work we wanted to show particularly whether and how the diol and the proline moiety has an effect on the chromophoric π-electron system as an result of interactions with the surroundings of the molecules. It is to clarify, what proportions of these environment effects are dipole–dipole and/or hydrogen bond or acid–base interactions. By use of LSER (eqn (1a)) the individual solvation effects between the probe (**2a**, **2c**) and the solvent can be described and separated. The empirical solvent parameters of Kamlet–Taft and Catalán can thus be compared.

Results and discussion

Synthesis

The nucleophilic aromatic substitution of activated fluoroaromatics with amines provides an easy route to the synthesis of new donor–acceptor-substituted chromophores.[17] The most frequently used procedure for the synthesis of chromophoric azo dyes, the coupling of diazotized aromatic amines with electron-rich aromatics, cannot be used for the synthesis of fluorine-functionalized azo substances. Electron-poor azo aromatics are, however, accessible *via* azo condensation. In this work, we used the nucleophilic aromatic substitution of highly active fluoroaromatics **1** described by Neunhoeffer *et al.*, who were compelled to replace 2,4-dinitrofluorobenzene (DNFB) by compound **1**, which, like the Sanger reagent, had a readily substituted fluorine atom. However, the chromophoric group needed to be present in the molecule at the same time, and this leads to deeply colored derivatives, compared with dinitrophenylamino acids, which are easier to determine colorimetrically. The reaction with various amines and amino acids showed that the colorimetric determination is approximately 100 times more sensitive than that of the known DNFB derivatives.[13] The NMR spectroscopic data for **1** have not previously been described.

Compounds **2a–c** are obtained under mild conditions (room temperature, $NaHCO_3$-containing medium) by nucleophilic aromatic substitution of **1** with the corresponding amines (Scheme 1).

Single-crystal X-ray structure analysis

Crystals of **2a** suitable for single-crystal X-ray structure analysis have been obtained by slow diffusion of *n*-hexane into an acetone solution of **2a**. Compound **2a** crystallizes in the triclinic space group $P\bar{1}$ with one acetone molecule connected *via* a hydrogen bridge (O5–H5O···O9, 2.739(2) Å). The molecular structure of that aggregate is shown in Fig. 1, giving the atomic labeling. The crystallographic data and collection parameter as well as bond lengths and angles are provided as ESI.†

Compound **2a** posses in the solid state *trans*-configuration with respect to the N=N double bond, as typically observed for azo compounds.[18] The azobenzene unit together with the nitro groups N1,O1,O2 and N6,O7,O8 is almost coplanar whereby the nitro group *ortho* to the azo group is pushed out of the plane. As expected, there is an intramolecular hydrogen bond between the amino proton and the *ortho*-nitro group (N5–H5N···O7, 2.639(2) Å).[18] In the solid state, dimers are formed by intermolecular hydrogen bonding between the diol groups (O6–H6O···O5A, 2.767(2) Å) with the additional "A" letter invoking symmetry operation $(2 - x, 1 - y, 1 - z)$. In addition, π–π stacking interactions between the nitro-functionalized azobenzene units are observed, giving rise to the formation of 2D-layers (Fig. 2).

Solvent effects on the UV/Vis absorption spectra

The new dyes **2a–c** were investigated for their activity as solvent-sensitive indicators.

UV/Vis spectroscopic investigations on **2b** indicate a self aggregation behavior. It is known that intermolecular hydrogen bonds exist between carboxylic acid molecules and this aggregation is dependent on parameters such as concentration of the acid, temperature and solvent polarity.[15,19] In a concentration range of $(2.514–0.402) \times 10^{-5}$ M the UV/Vis absorption maximum of **2b** in methanol undergoes a bathochromic shift from λ_{max} = 463 to 469 nm. Since the aggregation behavior of **2b** and analogous solvatochromic chromophores containing carboxylic acid groups in protic solvents is not yet fully understood,[15] compound **2b** was not investigated further with regard to its solvatochromic behavior.

Concentration-dependent UV/Vis spectroscopic investigations of compounds **2a** and **2c** did not show a shift of the UV/Vis absorption maxima. Compounds **2a** and **2c**, which thus do not self-aggregate can be investigated with regard to their

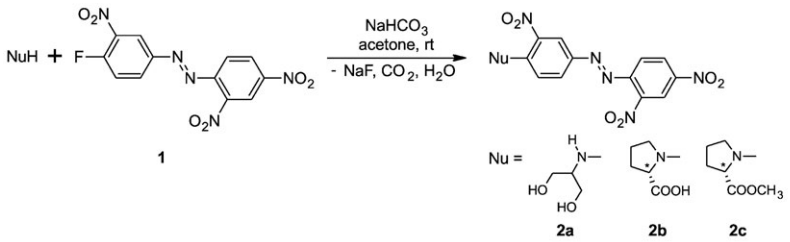

Scheme 1 Synthesis of compounds **2a–c** by nucleophilic aromatic substitution of the fluoroazo dye **1** with 2-aminopropane-1,3-diol, (*S*)-proline and (*S*)-proline methyl ester.

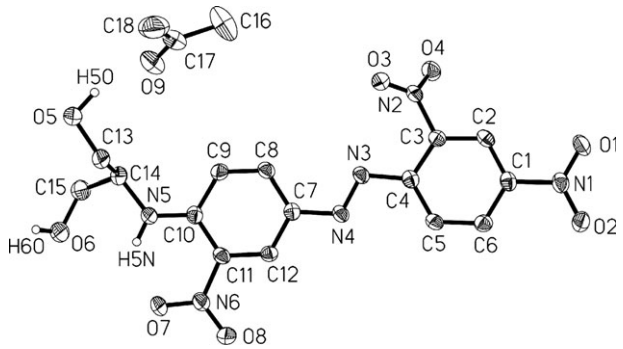

Fig. 1 ORTEP of the molecular structure of **2a** with displacement ellipsoids shown at 50% probability level.

solvatochromic properties. Table 1 shows the UV/Vis absorption maxima of **2a** and **2c** in a variety of solvents.

The substances show the shortest wavelength shift in 1,1,1,3,3,3-hexafluoro-2-propanol (λ_{max}(**2a**) = 408 nm) and in 2,2,2-trifluoroethanol (λ_{max}(**2c**) = 429 nm). Dye **2a** exhibits the largest bathochromic shift of the UV/Vis absorption maximum λ_{max} in triethylamine (λ_{max}(**2a**) = 442 nm). On the other hand compound **2c** shows the longest wavelength absorption band in the solvent dimethyl sulfoxide (DMSO) (λ_{max}(**2c**) = 459 nm). These shifts correspond to a positive solvatochromism with a solvatochromic range of $\Delta\tilde{\nu}$(**2a**) = 1890 cm^{-1} and $\Delta\tilde{\nu}$(**2c**) = 1520 cm^{-1}. Because of the strong electron-donating proline substituents, compound **2c** always absorbs at a longer wavelength than compound **2a** (Fig. 3).

The UV/Vis absorption bands of **2a** in pyridine, *N*,*N*-dimethylacetamide, *N*,*N*-dimethylformamide (DMF) and DMSO (HBA solvents, higher dipolarity/polarizability term) exhibit an unsymmetrical band shape with a bathochromic shoulder toward the UV/Vis absorption maximum.

Solvatochromic measurements were therefore carried out in room temperature ionic liquids (RTILs) (Table 2). For the investigations we chose the 1-butyl-3-methylimidazolium salts $[C_4\text{-mim}]^+$ with $[Cl]^-$ and the weakly coordinating $[PF_6]^-$ und $[BF_4]^-$ anions. Variation of the anion offers the possibility of varying the HPA capacity of the RTIL, which generally shows a higher dipolarity/polarizability term. In particular $[C_4\text{-mim}][Cl]$ allows the use of the solvent with a high β value.

The UV/Vis absorption spectra of **2a** and **2c** show, as expected, a bathochromic shift from $[C_4\text{-mim}][PF_6]$ to $[C_4\text{-mim}][Cl]$ with increasing capacity of the anion of the ionic liquid to act as a hydrogen bond acceptor (HBA) or electron pair donor (EPD). The UV/Vis absorption bands of **2a** have an unsymmetrical band shape because of a bathochromic shoulder to the UV/Vis absorption maximum.

LSE correlation analyses

The position of the UV/Vis absorption maxima of **2a** and **2c** with regard to dipolarity/polarizability (π^*, *SPP* and *SP*, respectively) and hydrogen bonding capacity (α, β, *SA* and

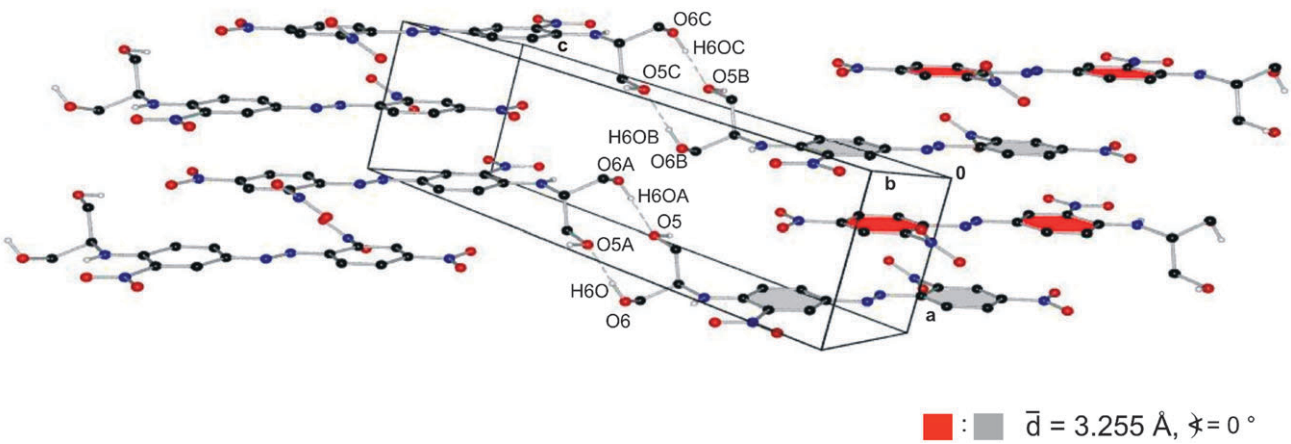

Fig. 2 Part of the 2D-layer of **2a** formed in the solid state due to hydrogen bonding between diol moieties and π–π interactions with $\bar{d}$ giving the average distance of the aromatic units and ∢ giving the interplanar angle of adjacent aromatic units. The acetone molecules as non-interacting packing solvents have been omitted for clarity. The symmetry operations invoked by the A, B and C labels are $(2 - x, 1 - y, 1 - z)$, $(x - 1, y, z)$ and $(1 - x, 1 - y, 1 - z)$, respectively.

Table 1 UV/Vis absorption maxima of **2a** and **2c** measured in 28 solvents of different polarity and hydrogen bond ability

	$10^{-3}\tilde{\nu}_{max}/cm^{-1}$	
Solvent	**2a**	**2c**
Triethylamine	22.62	22.42
Tetrachloromethane	[a]	22.22
Toluene	23.15	22.22
Benzene	23.15	22.22
Diethyl ether	23.26	22.62
1,4-Dioxane	23.20	22.47
Anisole	22.88	22.08
Tetrahydrofuran	23.09	22.22
Ethyl acetate	23.26	22.47
Chloroform	23.47	22.22
Pyridine	22.68	21.83
Dichloromethane	23.53	22.27
1,2-Dichloroethane	23.42	22.12
Benzonitrile	22.88	21.79
Acetone	23.53	22.47
N,*N*-Dimethylacetamide	23.04	21.98
N,*N*-Dimethylformamide	23.04	22.08
Dimethyl sulfoxide	23.04	21.79
Acetonitrile	23.58	22.52
Nitromethane	23.59	22.47
1-Decanol	22.78	22.22
1-Butanol	23.20	22.42
2-Propanol	23.31	22.57
1-Propanol	23.31	22.47
Ethanol	23.47	22.57
Methanol	23.75	22.73
2,2,2-Trifluoroethanol	24.39	23.31
1,1,1,3,3,3-Hexafluoro-2-propanol	24.51	23.26
$\Delta\tilde{\nu}/cm^{-1}$	1765	1520

[a] Probe is insoluble in this solvent.

SB, respectively) of the solvent can be interpreted using the Kamlet–Taft equation (simplified eqn (1b)) and the Catalán equations (eqn (1c) and (1d)).

$$\tilde{\nu}_{max} = \tilde{\nu}_{max,0} + a\alpha + b\beta + s\pi^* \quad (1b)$$

$$\tilde{\nu}_{max} = \tilde{\nu}_{max,0} + aSA + bSB + sSPP \quad (1c)$$

$$\tilde{\nu}_{max} = \tilde{\nu}_{max,0} + aSA + bSB + sSP \quad (1d)$$

The solvent parameters α,[8d] β,[8d] π^*,[8d] *SA*,[10a] *SB*,[10a] *SPP*[10a] and *SP*[10g] used for the multiple linear regression analysis are given in the ESI.† The regressions of **2a** and **2c** which are qualitatively the best according to the solvent scales of Kamlet–Taft and Catalán are shown in Table 3.

The Kamlet–Taft and Catalán solvent scales show clear differences with regard to the weighting of the individual solvent parameters, which are reflected in the correlations of **2a** and **2c** shown. Thus, for example, acetone has an α value of 0.08 and hence, shows a very low acidity.[8d] The *SA* scale shows, however, a value of 0, through which acetone is estimated to be a weaker hydrogen bond donor than, for example, pyridine, 1,2-dichloroethane or benzonitrile.[10a] Differences between the scales are also clear for the hydrogen bond acceptor capacity (HBA ability). In comparison with triethylamine (β = 0.71),[8d] according to Kamlet–Taft, 1-propanol (β = 0.90)[8d] is classified as a stronger hydrogen bond acceptor. On the other hand Catalán classifies triethylamine (*SB* = 0.885)[10a] as having a clearly higher affinity to accept hydrogen bonds than 1-propanol (*SB* = 0.782).[10a] Further examples of such an inversion have been established between *N*,*N*-dimethylacetamide and DMSO (ESI,† Table S1).[8d,10a] Furthermore, there are also significant differences in the dipolarity/polarizability terms. With a π^* value of 0.73[8d] 2,2,2-trifluoroethanol (TFE) and anisole are estimated to be the same, although the dipole moment of TFE is almost double that of anisole (μ_{TFE} = 2.46 D, $\mu_{anisole}$ = 1.26 D).[21] While the *SPP* parameters of the solvents are of the same order of magnitude (SPP_{TFE} = 0.908, $SPP_{anisole}$ = 0.823),[10a] the *SP* parameters clearly differ significantly. Thus anisole with *SP* = 0.8204[10g] has a significantly higher value than TFE (SP_{TFE} = 0.5431).[10g]

The results of the regressions of **2a** and **2c** show that the LSERs according to Catalán are most significant with the parameters *SA*, *SB* and *SP* having the greatest significance ($r > 0.90$). Unlike the multiple linear regression analysis of **2a** taking into account the polarizability of the solvent (*SP* value), the correlation coefficient becomes markedly smaller with regard to π^* and *SPP*. The correlation of **2a** and **2c** taking into account the *SP* value shows as well that the absolute *s* value is significantly greater than the coefficients *a* and *b*. This shows that the UV/Vis absorption spectrum is more strongly dependent on the change in the polarizability of the chromophore surroundings than on the capacity of the solvent to act as a hydrogen bond donor or acceptor.

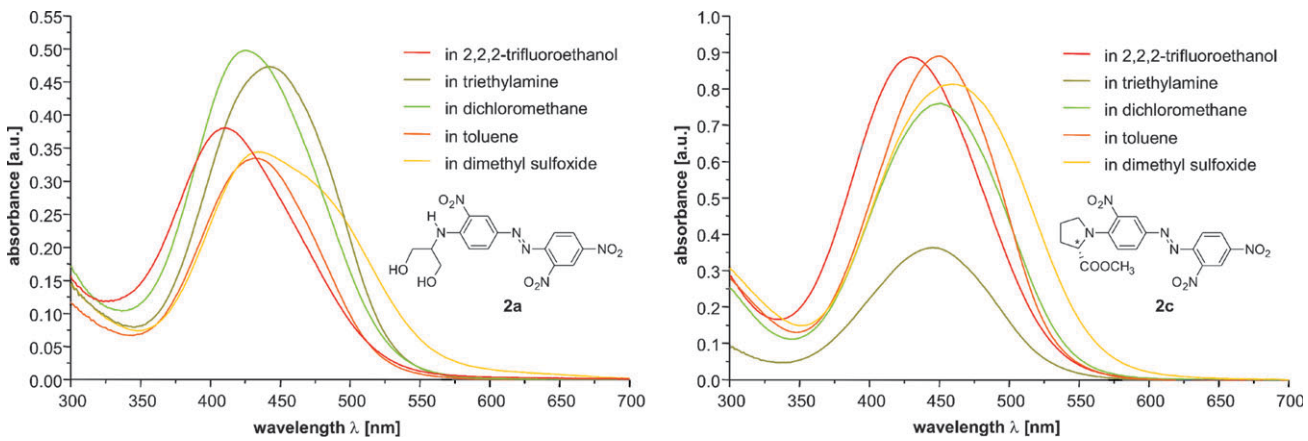

Fig. 3 UV/Vis absorption spectra of **2a** and **2c** in different solvents.

Table 2 UV/Vis absorption maxima of **2a** and **2c** measured in three RTILs[20]

	$10^{-3}\tilde{\nu}_{max}/cm^{-1}$		Kamlet–Taft parameters		
Ionic liquid	**2a**	**2c**	α	β	π^*
[C_4-mim][PF_6]	23.31	22.32	0.54	0.44	0.90
[C_4-mim][BF_4]	23.37	22.42	0.53	0.55	0.96
[C_4-mim][Cl]	22.73	21.79	0.31	0.95	1.13

Table 3 Solvent-independent correlation coefficients *a*, *b* and *s* of the Kamlet–Taft parameters α, β and π^* and Catalán parameters *SA*, *SB*, *SPP* and *SP*, respectively, solute property of the reference system $\tilde{\nu}_{max,0}$, significance (*f*), correlation coefficient (*r*), standard deviation (*sd*), and number of solvents (*n*) calculated for the solvatochromism of compounds **2a** and **2c**

Eqn	Compd.	$\tilde{\nu}_{max,0}$	*a*	*b*	*s*	*n*	*f*	*r*	*sd*
(1b)	**2a**	23.431 (±0.082)	0.591 (±0.080)	−0.729 (±0.141)	—	27	<0.0001	0.881	0.216
(1c)	**2a**	23.429 (±0.092)	1.143 (±0.210)	−0.712 (±0.174)	—	26	<0.0001	0.806	0.230
(1d)	**2a**	25.252 (±0.370)	0.540 (±0.168)	−0.912 (±0.116)	−2.694 (±0.467)	26	<0.0001	0.928	0.148
(1b)	**2c**	22.675 (±0.138)	0.517 (±0.069)	−0.345 (±0.121)	−0.529 (±0.176)	28	<0.0001	0.873	0.187
(1c)	**2c**	23.105 (±0.329)	1.113 (±0.196)	—	−1.123 (±0.400)	27	<0.0001	0.769	0.217
(1d)	**2c**	25.036 (±0.200)	0.235 (±0.091)	−0.352 (±0.060)	−3.594 (±0.254)	27	<0.0001	0.972	0.080

In the case of the calculated LSERs of **2c**, the solvent independent correlation coefficients *a*, *b* and *s* are all in the same area of magnitude, taking α, β and π^*, as well as *SA* and *SPP* into consideration. However, the correlation coefficients *r* obtained for **2c** are markedly less than 0.90, which strongly reduces the relevance of this correlation, when compared with the correlation taking *SP* into consideration.

Compound **2a** is able to form intramolecular hydrogen bonds to the *ortho*-nitro group[18c] because of the secondary amino functionality. Thus, the ability of the amino group in **2a** to form hydrogen bonds to the solvent would be about as small as in **2c**. The effect of the β term of the solvent on the shift of the λ_{max} of the azo dye **2a** is clearly greater than in **2c**. This strongly positive solvatochromic effect with regard to the HPA ability of the solvent can be justified on the one hand, in terms of a specific solvation of the diol unit by hydrogen bond formation. We found a similar effect of the β parameter in the solvatochromic investigations of *N*-(2-hydroxyethyl)-substituted Michler's ketones and *N*-(methyl-*N*-[1-(2,3-dihydroxypropyl)])-4-nitroaniline derivatives.[14a,22] On the other hand, **2a** shows the longest wavelength UV/Vis absorption band in the strongly hydrogen bond accepting solvent triethylamine (*SB* = 0.885). Unlike the high polarity HBA solvents (pyridine, *N*,*N*-dimethylacetamide, DMF and DMSO), a symmetrical band shape is obtained in triethylamine. This result is explained in terms of the specific interaction between the protons of the amino group of **2a** with the tertiary amine in competition with the intramolecular hydrogen bonding to the *ortho*-nitro group, which is correspondingly suppressed. In order to verify this, the UV/Vis absorption maximum of **2a** was determined in a further tertiary amine solvent. In triethylamine, compound **2a** also shows a symmetrical band with λ_{max} = 448 nm. The previously made predictions with regard to the possible interactions of **2a** with HBA solvents are therefore reinforced.

In all the regressions of **2a** and **2c** the correlation coefficients *b* and *s* are always negative, which corresponds to a bathochromic shift of λ_{max} with increasing hydrogen bond acceptor capacity or with the polarity of the solvent (positive solvatochromism). This allows one to conclude that the first excited state is more stabilized as a result of solvation than the ground state. The positive sign of the correlation coefficient *a* for both azo dyes **2a** and **2c** indicates a hypsochromic shift of λ_{max} with increasing hydrogen bond donor capacity of the solvent (negative solvatochromism). This suggests a stabilization of the ground state, compared with the first excited state.

Solvatochromic measurements in RTILs, which act as hydrogen bond acceptors and have a high dipolarity/polarizability term, confirm the differentiating solvatochromic behavior of **2a**

Table 4 Solvent-independent correlation coefficients *a*, *b* and *s* of the Kamlet–Taft parameters α, β and π^*, respectively, solute property of the reference system $\tilde{\nu}_{max,0}$, significance (*f*), correlation coefficient (*r*), standard deviation (*sd*), and number of solvents (*n*) calculated for the solvatochromism of compounds **2a** and **2c**

Eqn	Compd.	$10^{-3}\tilde{\nu}_{max,0}$	*a*	*b*	*s*	*n*	*f*	*r*	*sd*
(1b)	**2a**	23.442 (±0.077)	0.591 (±0.076)	−0.763 (±0.129)	—	30	<0.0001	0.885	0.206
(1b)	**2c**	22.686 (±0.117)	0.522 (±0.066)	−0.361 (±0.110)	−0.534 (±0.145)	31	<0.0001	0.878	0.181

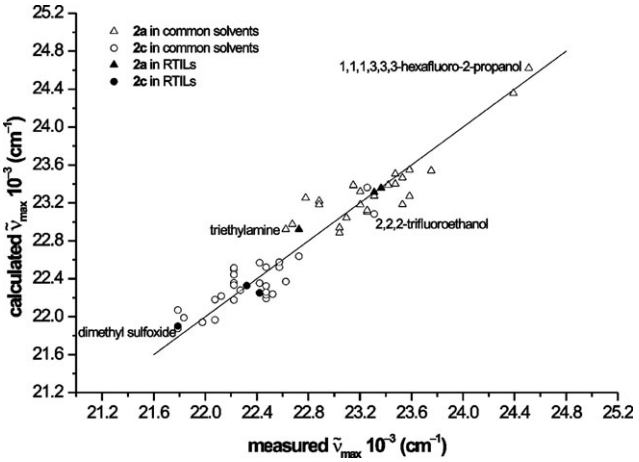

Fig. 4 Relationship between calculated and measured $\tilde{\nu}_{max}$ values for **2a** and **2c** according the Kamlet–Taft eqn (1a).

compared with HBA solvents with dipolarity/polarizability terms of differing strength (Table 4, Fig. 4).

Acidochromism

Azo dyes are known acid–base indicators, where the color reaction and hence the change in the UV/Vis absorption is attributed to a protonation equilibrium. The azo dyes have two possible positions for a protonation either the amino function or on the β-nitrogen of the azo group.[5b] The amino group serves as an electron donor; protonation at this position leads to a neutralization of the +M effect, and thus, to a loss of the push–pull character of the aromatic system. A hypsochromic shift in the UV/Vis absorption spectrum would therefore be evidence of this type of protonation. Such a shift was, however, not observed with **2a**, **2b** or **2c**, and can therefore be ruled out. A protonation on the β-nitrogen of the azo group leads to an increase in the −M effect of this group, whereby the aromatic push–pull system is reinforced. This results in a marked shift of the UV/Vis absorption maxima to longer wavelengths.

Compounds **2a–c** dissolve in 36% aqueous hydrochloric acid with an intense red color (λ_{max}(**2a**) = 537 nm, λ_{max}(**2b**) = 542 nm, λ_{max}(**2c**) = 543 nm). When the pH value is increased by addition of water, this UV/Vis absorption band is reduced, while at the same time, a new shorter wavelength band is formed (λ_{max}(**2a**) = 424 nm, λ_{max}(**2b**) = 448 nm, λ_{max}(**2c**) = 445 nm). An isosbestic point can thus be observed (λ_{isos}(**2a**) = 468 nm, λ_{max}(**2b**) = 479 nm, λ_{isos}(**2c**) = 477 nm). The position of the newly formed band is representative of the neutral form, as here the absorption maxima found are identical to those observed in the neutral comparison solvent acetone (λ_{max}(**2a**) = 424 nm, λ_{max}(**2b**) = 448 nm, λ_{max}(**2c**) = 445 nm). The investigations in aqueous media are, however, limited by the low solubility of the azo dyes (5–12 M HCl). For this reason we investigated the influence of the acid strength on the position on the UV/Vis absorption maxima (Fig. 5). In weak acids such as, for example, acetic acid (λ_{max}(**2a**) = 440 nm, λ_{max}(**2b**) = 436 nm, λ_{max}(**2c**) = 440 nm), or propionic acid (λ_{max}(**2a**) = 424 nm, λ_{max}(**2b**) = 437 nm, λ_{max}(**2c**) = 441 nm), where no protonation is observed, the azo dyes absorb in the same region as in acetone. On the other hand, marked differences are observed when formic acid is used. Compound **2a** absorbs in acetic acid at λ_{max} = 418 nm and shows a shoulder in the region around 500 nm. This is evidence of incomplete protonation. On the other hand, molecules **2b** and **2c** show a different pattern of absorption bands. **2b** and **2c** absorb in these medium strength acids with a very broad band, where the maxima are at λ_{max}(**2b**) = 513 nm and λ_{max}(**2c**) = 509 nm, respectively, and show a shoulder in the area of 450 nm. This points to a stronger protonation than in compound **2a**. The azo dyes tested show a bathochromic shift in trifluoroacetic acid, an example of a strong acid (λ_{max}(**2a**) = 523 nm, λ_{max}(**2b**) = 527 nm, and λ_{max}(**2c**) = 532 nm). The observed shift is, however, somewhat smaller on the basis of the reduced acid strength compared with concentrated

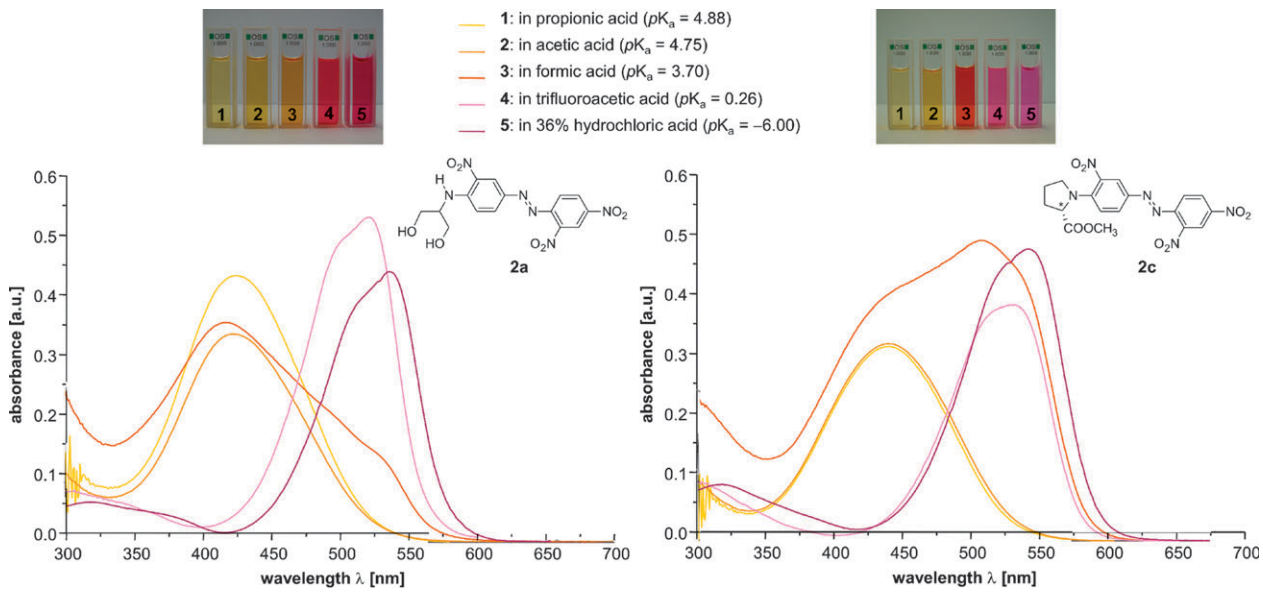

Fig. 5 UV/Vis absorption maxima of **2a** and **2c** measured in five acids of different pK_a values.[23]

hydrochloric acid. The difference in behavior compared with formic acid can be attributed to the different amino substituents. Proline (**2b**) or proline methyl ester (**2c**) as secondary amines have a stronger +M effect compared with the amino substituent of **2a**. In this respect, the β-nitrogen of the azo group is more nucleophilic and is more easily accessible for protonation.

Conclusions

The new azo dyes 2-({4-[(*E*)-(2,4-dinitrophenyl)diazenyl]-2-nitrophenyl}amino)propane-1,3-diol (**2a**), (2*S*)-1-{4-[(*E*)-(2,4-dinitrophenyl)diazenyl]-2-nitrophenyl}pyrrolidine-2-carboxylic acid (**2b**) and methyl-(2*S*)-1-{4-[(*E*)-(2,4-dinitrophenyl)diazenyl]-2-nitrophenyl}pyrrolidine-2-carboxylate (**2c**) were synthesized *via* nucleophilic aromatic substitution of the fluoro-functionalized azo dye (*E*)-1-(2,4-dinitrophenyl)-2-(4-fluoro-3-nitrophenyl)-diazene (**1**) with 2-aminopropane-1,3-diol, (*S*)-proline and (*S*)-proline methyl ester. The structure of **2a** in the solid state was determined. This shows the formation of a dimer. The solvatochromic behavior of dyes **2a** and **2c** was investigated in 31 solvents of differing acidity, basicity and polarity. The individual solute/solvent interactions were described with the aid of LSER correlations. As well as the established analysis according to Kamlet–Taft, the newer solvent parameters of Catalán were applied. The results of the multiple linear correlation analyses led to the conclusion that the influence of the polarizability of the solvent is the most dominant effect on the UV/Vis absorption maxima of **2a** and **2c**. The effect of the acidity and/or basicity of the solvent is marginal compared with the effect of *SP*. The influence of the acid strength on the protonation of the azo dyes **2a–c** was investigated in five different acids with various pK_a values. Strong acids preferentially protonate the nitrogen in the β-position of the azo group, whereas no protonation was observed with weak acids. UV/Vis spectroscopic differences between **2a** and **2b/c** were evident, when formic acid was used, in that the UV/Vis absorption maximum of compounds **2b** and **2c** showed a bathochromic shift compared with **2a**.

Experimental

General

Solvents (Merck, Fluka, Lancaster and Aldrich) were redistilled over appropriate drying agents prior to use. All commercial reagents were used without further purification. They were purchased from the following supplier: Merck: (*S*)(−)-proline (≥ 99%); Fluka: (*S*)(−)-proline methyl ester hydrochloride (≥ 99%), 2-aminopropane-1,3-diol (97%).

All melting points (mp) were measured on a Boetius melting point apparatus and were uncorrected. The UV/Vis absorption spectra were obtained with an MCS 400 diode array UV/Vis spectrometer from Carl Zeiss, Jena, connected *via* glass-fibre optics. ^{1}H and ^{13}C NMR spectra were measured at 20 °C on a Bruker Advance 250 NMR spectrometer at 250 and 69.9 MHz. The residue signals of the solvents (DMSO-d_6) were used as internal standards. The solid-state ^{13}C{^{1}H} CP-MAS NMR experiments (100.6 MHz) were recorded on a Bruker Digital Avance 400 spectrometer equipped with 7-mm double-tuned probes capable of MAS at 12 kHz. Data acquisition was performed with proton decoupling (TPPM). NMR spectra were referenced to adamantane (δ = 38.5 ppm). The FT-IR spectra were measured by means of diffuse reflection diluted with KBr at room temperature in the wavenumber range from 400 to 4000 cm^{-1} on a Perkin-Elmer Fourier transform 1000 spectrometer. Elemental analysis was determined with a Vario-EL analyser.

Correlation Analysis: Multiple regression analysis was performed with the Origin 5.0 statistics program.

Syntheses

(*E*)-1-(2,4-Dinitrophenyl)-2-(4-fluoro-3-nitrophenyl)diazene (1). Compound **1** was prepared as described in the literature.[13]

Orange solid. 72% yield. Mp 152 °C (lit.,[13] 152−153 °C). ^{1}H NMR (250 MHz, DMSO-d_6, 25 °C): δ 7.89 (1 H, dd, ^3J = 8.9 Hz, $^3J_{FH}$ = 10.7 Hz, ArH) 7.93 (1 H, d, ^3J = 8.8 Hz, ArH), 8.37 (1 H, ddd, ^3J = 8.9 Hz, ^4J = 2.5 Hz, $^4J_{FH}$ = 4.1 Hz, ArH), 8.61 (1 H, dd, ^4J = 2.5 Hz, $^4J_{FH}$ = 7.1 Hz, ArH), 8.70 (1 H, dd, ^3J = 8.8 Hz, ^4J = 2.4 Hz, ArH), 9.00 (1 H, d, ^4J = 2.4 Hz, ArH). ^{13}C NMR (69.9 MHz, DMSO-d_6, 25 °C): δ 120.25 ($^2J_{C,F}$ = 22.1 Hz), 120.36, 120.42, 120.81 ($^3J_{C,F}$ = 1.9 Hz), 128.85, 130.83 ($^3J_{C,F}$ = 10.1 Hz), 137.82 ($^2J_{C,F}$ = 9.1 Hz), 146.07, 147.02, 147.41 ($^4J_{C,F}$ = 3.4 Hz), 148.18, 157.04 ($^1J_{C,F}$ = 269.7 Hz). IR (KBr): $\tilde{\nu}$/cm^{-1} = 3106, 1609, 1535, 1364, 1259. Anal. Calc. for $C_{15}H_{14}N_6O_8$: C, 43.00; H, 1.80; N, 20.89. Found: C, 42.87; H, 2.15; N, 20.45%.

2-({4-[(*E*)-(2,4-Dinitrophenyl)diazenyl]-2-nitrophenyl}amino)-propane-1,3-diol (2a). 2-Aminopropane-1,3-diol (0.035 g, 0.386 mmol), $NaHCO_3$ (0.065 g, 0.772 mmol) and (*E*)-1-(2,4-dinitrophenyl)-2-(4-fluoro-3-nitrophenyl)diazene **1** (0.129 g, 0.386 mmol) were dissolved in 50 mL of acetone and the reaction mixture was stirred for 48 h at room temperature. It was poured into 50 mL of water and neutralized with 1 M HCl. The resulting red precipitate was recovered by filtration and washed with water to give **2a** (0.113 g, 0.279 mmol) as a red solid. 73% yield. Mp 190 °C. ^{1}H NMR (250 MHz, DMSO-d_6, 25 °C): δ 3.62–3.67 (4 H, m, CH_2), 3.96–3.99 (1 H, m, CH), 5.11 (2 H, t, ^3J = 5.5 Hz, OH), 7.42 (1 H, d, ^3J = 9.6 Hz, ArH), 7.96 (2 H, m, ArH), 8.60 (1 H, dd, ^3J = 8.8 Hz, ^4J = 2.1 Hz, ArH), 8.69 (1 H, d, ^4J = 2.4 Hz, ArH), 8.94 (1 H, d, ^3J = 2.1 Hz, ArH), 9.01 (1 H, d, ^3J = 8.5 Hz, NH). ^{13}C CP MAS NMR (400 MHz, 12 kHz, 25 °C): δ 57.3, 60.5, 61.5, 114.6, 119.3, 124.2, 126.6, 130.5, 134.1, 139.2, 144.7, 146.8, 147.1, 149.1. IR (KBr): $\tilde{\nu}$/cm^{-1} = 3400, 3324, 3095, 2948, 1615, 1566, 1528, 1430, 1339. Anal. Calc. for $C_{15}H_{14}N_6O_8$: C, 44.34; H, 3.47; N, 20.68. Found: C, 44.32; H, 3.37; N, 20.37%. UV/Vis: λ_{max}-(MeOH)/nm 423 (ε/L mol^{-1} cm^{-1} 34 100), λ_{max}(HCl)/nm 537 (ε/L mol^{-1} cm^{-1} 59 700).

(2*S*)-1-{4-[(*E*)-(2,4-Dinitrophenyl)diazenyl]-2-nitrophenyl}-pyrrolidine-2-carboxylic acid (2b). (*S*)-Proline (0.150 g, 1.303 mmol) and $NaHCO_3$ (0.219 g, 2.606 mmol) were dissolved in 20 mL of water. To this solution was added (*E*)-1-(2,4-dinitrophenyl)-2-(4-fluoro-3-nitrophenyl)diazene **1** (0.437 g, 1.303 mmol) dissolved in 35 mL of acetone. The reaction mixture was stirred for 48 h at room temperature and then poured into 50 mL 2 M HCl. The resulting red precipitate was

recovered by filtration and washed with water to give **2b** (0.395 g, 0.918 mol) as a red solid. 70% yield. Mp 138 °C. ^{1}H NMR (250 MHz, DMSO-d_6, 25 °C): δ 1.87–2.08 (3 H, m, proH-3/4), 2.45–2.50 (1 H, m, proH-3 or proH-4), 3.17–3.49 (2 H, m, proH-5), 4.61–4.67 (1 H, m, proH-2), 7.12 (1 H, d, ^3J = 9.3 Hz, ArH), 7.90 (1 H, d, ^3J = 8.9 Hz, ArH), 7.96 (1 H, dd, ^3J = 9.3 Hz, ^4J = 2.4 Hz, ArH), 8.32 (1 H, d, ^4J = 2.4 Hz, ArH), 8.60 (1 H, dd, ^3J = 8.9 Hz, ^4J = 2.5 Hz, ArH), 8.93 (1 H, d, ^4J = 2.5 Hz, ArH), 13.17 (1 H, s, COOH). ^{13}C CP MAS NMR (400 MHz, 12 kHz, 25 °C): δ 26.4, 31.1, 52.8, 64.2, 114.7, 118.9, 129.1, 135.7, 137.9, 141.8, 146.0, 180.6. IR (KBr): $\tilde{\nu}$/cm^{-1} = 3626, 3104, 2986, 2885, 1727, 1605, 1530, 1345, 1294, 1158, 1060, 836. Anal. Calc. for $C_{17}H_{14}N_6O_8$: C, 47.45; H, 3.28; N, 19.53. Found: C, 47.37; H, 3.45; N, 19.61%. UV/Vis: λ_{max}(HCl)/nm 542 (ε/L mol^{-1} cm^{-1} 41 700).

Methyl-(2*S*)-1-{4-[(*E*)-(2,4-dinitrophenyl)diazenyl]-2-nitrophenyl}pyrrolidine-2-carboxylate (2c). (*S*)-Proline methyl ester hydrochloride (0.247 g, 1.492 mmol) and $NaHCO_3$ (0.251 g, 2.984 mmol) were dissolved in 20 mL of water. To this solution was added (*E*)-1-(2,4-dinitrophenyl)-2-(4-fluoro-3-nitrophenyl)diazene **1** (0.500 g, 1.492 mmol) dissolved in 35 mL of acetone. The reaction mixture was stirred for 48 h at room temperature and then poured into 50 mL 2 M HCl. The resulting red precipitate was recovered by filtration and washed with water to give **2c** (0.517 g, 1.164 mol) as a dark-red solid. 78% yield. Mp 244 °C. ^{1}H NMR (250 MHz, DMSO-d_6, 25 °C): δ 1.84–2.09 (3 H, m, proH-3/4), 2.39–2.47 (1 H, m, proH-3 or proH-4), 3.19–3.27 (1 H, m, proH-5a), 3.39–3.50 (1 H, m, proH-5b), 3.69 (3 H, s, $COOCH_3$), 4.74–4.79 (1 H, m, proH-2), 7.11 (1 H, d, ^3J = 9.4 Hz, ArH), 7.91 (1 H, d, ^3J = 8.9 Hz, ArH), 7.95 (1 H, dd, ^3J = 9.4 Hz, ^4J = 2.3 Hz, ArH), 8.34 (1 H, d, ^4J = 2.3 Hz, ArH), 8.61 (1 H, dd, ^3J = 8.9 Hz, ^4J = 2.4 Hz, ArH), 8.94 (1 H, d, ^4J = 2.4 Hz, ArH). ^{13}C NMR (69.9 MHz, DMSO-d_6, 25 °C): δ 24.2, 30.1, 51.9, 52.5, 61.9, 118.0, 119.8, 120.1, 125.1, 125.8, 128.2, 136.7, 141.7, 144.5, 146.2, 147.0, 147.2, 171.3. IR (KBr): $\tilde{\nu}$/cm^{-1} = 3102, 2956, 2882, 1746, 1602, 1520, 1341, 1153, 1061, 832. Anal. Calc. for $C_{18}H_{16}N_6O_8$: C, 48.65; H, 3.63; N, 18.91. Found: C, 48.21; H, 3.67; N, 18.58. UV/Vis: λ_{max}(MeOH)/nm 440 (ε/L mol^{-1} cm^{-1} 26 500), λ_{max}(HCl)/nm 543 (ε/L mol^{-1} cm^{-1} 53 300).

Crystal data and structure refinement for compound 2a. Data collection were performed at 100 K on a Oxford Gemini diffractometer equipped with a graphite monochromator utilizing Cu-Kα radiation (λ = 1.54184 Å). The structure was solved by direct methods using SHELXS-97[24] and refined by full-matrix least-square procedures on F^2, using SHELXL-97.[25] Non hydrogen atoms were refined anisotropically. All hydrogen atoms were added on calculated positions, except for OH and NH protons which were found in difference Fourier synthesis.

$C_{18}H_{20}N_6O_9$, M = 464.40, crystal size 0.2 × 0.2 × 0.01 mm, triclinic, $P\bar{1}$, a = 6.7800(10), b = 8.0970(8), c = 19.7070(16) Å, V = 1068.0(2) Å^3, Z = 2, D_c = 1.444 Mg m^{-3}, 7626 reflections collected in the 4.54–60.46° θ range, 3106 unique (R_{int} = 0.0194) which were used in all calculations. The final $wR(F^2)$ was 0.0917 (all data).

Acknowledgements

Financial support by the DFG and the Fonds der Chemischen Industrie is gratefully acknowledged. We thank Prof. Dr. S. Reißmann, FSU Jena, for helpful discussions.

References

1 (*a*) J.-A. He, S. Bian, L. Li, J. Kumar and S. K. Tripathy, *J. Phys. Chem. B*, 2000, **104**, 10513; (*b*) Y. Li, Y. Deng, Y. He, X. Tong and X. Wang, *Langmuir*, 2005, **21**, 6567; (*c*) P. Che, Y. He and X. Wang, *Macromolecules*, 2005, **38**, 8657; (*d*) F. Chaput, D. Riehl, Y. Lévy and J.-P. Boilot, *Chem. Mater.*, 1993, **5**, 589; (*e*) S. Xie, A. Natansohn and P. Rochon, *Macromolecules*, 1994, **27**, 1489.

2 (*a*) Y. Wu, Q. Zhang, A. Kanazawa, T. Shiono, T. Ikeda and Y. Nagase, *Macromolecules*, 1999, **32**, 3951; (*b*) N. B. Holland, T. Hugel, G. Neuert, A. Cattani-Scholz, C. Renner, D. Oesterhelt, L. Moroder, M. Seitz and H. E. Gaub, *Macromolecules*, 2003, **36**, 2015; (*c*) D. K. Hore, A. L. Natansohn and P. L. Rochon, *J. Phys. Chem. B*, 2003, **107**, 2506.

3 (*a*) F. Ciuchi, A. Mazzulla, G. Carbone and G. Cipparrone, *Macromolecules*, 2003, **36**, 5689; (*b*) E. Hattemer, R. Zentel, E. Mecher and K. Meerholz, *Macromolecules*, 2000, **33**, 1972.

4 (*a*) X. Wang, J. Kumar, S. K. Tripathy, L. Li, J.-I. Chen and S. Marturunkakul, *Macromolecules*, 1997, **30**, 219; (*b*) X. Wang, K. Yang, J. Kumar, S. K. Tripathy, K. G. Chittibabu, L. Li and G. Lindsay, *Macromolecules*, 1998, **31**, 4126; (*c*) S. Balasubramanian, X. Wang, H. C. Wang, K. Yang, J. Kumar and S. K. Tripathy, *Chem. Mater.*, 1998, **10**, 1554; (*d*) O. Varnavski, R. G. Ispasoiu, M. Narewal, J. Fugaro, Y. Jin, H. Pass and T. Goodson III, *Macromolecules*, 2000, **33**, 4061; (*e*) G. Rojo, G. Martin, F. Agulló-López, G. A. Carriedo, F. J. García Alonso and J. I. Fidalgo Martinez, *Chem. Mater.*, 2000, **12**, 3603; (*f*) D. Kuciauskas, M. J. Porsch, S. Pakalnis, K. M. Lott and M. E. Wright, *J. Phys. Chem. B*, 2003, **107**, 1559.

5 (*a*) H. Beyer and W. Walter, in *Handbook of Organic Chemistry*, Prentice Hall, New York, 1996; (*b*) H. Zollinger, in *Color Chemistry, Syntheses, Properties, and Applications of Organic Dyes and Pigments*, VCH, Weinheim, 2nd edn, 1991.

6 (*a*) P. Uznanski and J. Pecherz, *J. Appl. Polym. Sci.*, 2002, **86**, 1459; (*b*) C. Egami, Y. Suzuki, O. Sugihara, H. Fujimura and N. Okamoto, *Jpn. J. Appl. Phys.*, 1997, **36**, 2902; (*c*) C. Rottman, A. Turniansky and D. Avnir, *J. Sol–Gel Sci. Technol.*, 1998, **13**, 17; (*d*) T. P. Jones and M. D. Porter, *Anal. Chem.*, 1988, **60**, 404; (*e*) I. M. Klotz and W.-C. Loh Ming, *J. Am. Chem. Soc.*, 1953, **75**, 4159; (*f*) A. S. Abd-El-Aziz, R. M. Okasha, T. H. Afifi and E. K. Todd, *Macromol. Chem. Phys.*, 2003, **204**, 555.

7 (*a*) M. G. Hutchings, P. Gregory, J. S. Campbell, A. Strong, J.-P. Zamy, A. Lepre and A. Mills, *Chem.–Eur. J.*, 1997, **3**, 1719; (*b*) D. Keil, H. Hartmann, I. Zug and A. Schroeder, *J. Prakt. Chem.*, 2000, **342**, 169; (*c*) E. Buncel and S. Rajagopal, *J. Org. Chem.*, 1989, **54**, 798; (*d*) E. Buncel and S. Rajagopal, *Acc. Chem. Res.*, 1990, **23**, 226; (*e*) A. Painelli, F. Terenziani, L. Angiolini, T. Benelli and L. Giorgini, *Chem.–Eur. J.*, 2005, **11**, 6053; (*f*) Y. Li, Z.-Y. Lin and W.-T. Wong, *Eur. J. Inorg. Chem.*, 2001, 3163.

8 (*a*) C. Reichardt, in *Solvents and Solvent Effects in Organic Chemistry*, VCH, Weinheim, 2nd edn, 1988, and references therein; (*b*) C. Reichardt, *Chem. Rev.*, 1994, **94**, 2319; (*c*) P. Müller, *Pure Appl. Chem.*, 1994, **66**, 1077; (*d*) Y. Marcus, *Chem. Soc. Rev.*, 1993, **22**, 409; (*e*) V. Gutmann, *Coord. Chem. Rev.*, 1976, **18**, 225; (*f*) V. Gutmann, in *The Donor–Acceptor Approach to Molecular Interactions*, Plenum Press, New York, 1978; (*g*) E. M. Kosower, *J. Am. Chem. Soc.*, 1958, **80**, 3253; (*h*) K. Dimroth, C. Reichardt, T. Siepmann and F. Bohlmann, *Justus Liebigs Ann. Chem.*, 1963, **661**, 1; (*i*) L. G. S. Brooker, A. C. Craig, D. W. Heseltine, P. W. Jenkins and L. L. Lincoln, *J. Am. Chem. Soc.*, 1965, **87**, 2443.

9 (*a*) R. W. Taft and M. J. Kamlet, *J. Am. Chem. Soc.*, 1976, **98**, 2886; (*b*) M. J. Kamlet and R. W. Taft, *J. Am. Chem. Soc.*, 1976, **98**, 377; (*c*) M. J. Kamlet, T. N. Hall, J. Boykin and R. W. Taft, *J. Org. Chem.*, 1979, **44**, 2599; (*d*) M. J. Kamlet, J.-L. M. Abboud

and R. W. Taft, *J. Am. Chem. Soc.*, 1977, **99**, 6027; (*e*) M. J. Kamlet, J.-L. M. Abboud, M. H. Abraham and R. W. Taft, *J. Org. Chem.*, 1983, **48**, 2877.
10 (*a*) J. Catalán, in *Handbook of Solvents*, ed. G. Wypch, ChemTech Publishing, Toronto, 2001, p. 583, ch. 9.3; (*b*) J. Catalán and C. Díaz, *Liebigs Ann./Recueil*, 1997, 1941; (*c*) J. Catalán and C. Díaz, *Eur. J. Org. Chem.*, 1999, 885; (*d*) J. Catalán, C. Díaz, V. López, P. Pérez, J.-L. G. de Paz and J.-G. Rodríguez, *Justus Liebigs Ann.*, 1996, 1785; (*e*) J. Catalán, V. López and P. Pérez, *Justus Liebigs Ann.*, 1995, 793; (*f*) J. Catalán, V. López, P. Pérez, R. Martín-Villamil and J.-G. Rodríguez, *Justus Liebigs Ann.*, 1995, 241; (*g*) J. Catalán and H. Hopf, *Eur. J. Org. Chem.*, 2004, 4694.
11 *CRC Handbook of Chemistry and Physics*, ed. D. R. Lide, CRC Press, Boca Raton, FL, 75th edn, 1994: *cf.* T. Abe, *Bull. Chem. Soc. Jpn.*, 1990, **63**, 2328.
12 M. Bauer, A. Rollberg, A. Barth and S. Spange, *Eur. J. Org. Chem.*, 2008, 4475.
13 O. Neunhoeffer and W. Ruske, *Justus Liebigs Ann.*, 1957, **610**, 143.
14 (*a*) S. Spange, K. Hofmann, B. Walfort, T. Rüffer and H. Lang, *J. Org. Chem.*, 2005, **70**, 8564; (*b*) A. Oehlke, A. A. Auer, I. Jahre, B. Walfort, T. Rüffer, P. Zoufalá, H. Lang and S. Spange, *J. Org. Chem.*, 2007, **72**, 4328.
15 K. Schreiter and S. Spange, *J. Phys. Org. Chem.*, 2008, **21**, 242.
16 S. M. B. Fraga, M. S. T. Gonçalves, J. C. V. P. Moura and K. Rani, *Eur. J. Org. Chem.*, 2004, 1750.
17 (*a*) J. F. Bunett and R. E. Zahler, *Chem. Rev.*, 1951, **49**, 273; (*b*) J. Sauer and R. Huisgen, *Angew. Chem.*, 1960, **72**, 294; (*c*) G. H. Schmid, in *Organic Chemistry*, Mosby-Verlag, St. Louis, 1st edn, 1996; (*d*) H. Suhr, *Chem. Ber.*, 1964, **97**, 3277; (*e*) H. Suhr, *Liebigs Ann. Chem.*, 1965, **687**, 175; (*f*) H. Suhr, *Liebigs Ann. Chem.*, 1965, **689**, 109; (*g*) H. Suhr, *Chem. Ber.*, 1964, **97**, 3268; (*h*) H. Grube and H. Suhr, *Chem. Ber.*, 1969, **102**, 1570.
18 (*a*) T. Yokoyama, *Aust. J. Chem.*, 1976, **29**, 1469; (*b*) T. Yokoyama, R. W. Taft and M. J. Kamlet, *Aust. J. Chem.*, 1983, **36**, 701; (*c*) R. Cattana, J. J. Silber and J. Anunziata, *Can. J. Chem.*, 1992, **70**, 2677.
19 (*a*) J. T. Bulmer and H. F. Shurvell, *J. Phys. Chem.*, 1973, **77**, 256; (*b*) N. Tanaka, H. Kitano and N. Ise, *J. Phys. Chem.*, 1990, **94**, 6290; (*c*) F. Laborie, *J. Polym. Sci.*, 1977, **15**, 1255; (*d*) T. Kuppens, W. Herrebout, B. Veken and P. Bultnick, *J. Phys. Chem. A*, 2006, **110**, 10191; (*e*) I. Wolfs and H. O. Desseyn, *J. Mol. Struct. (THEOCHEM)*, 1996, **360**, 81.
20 R. Lungwitz and S. Spange, *New J. Chem.*, 2008, **32**, 392.
21 A. L. McClellan, in *Tables of Experimental Dipole Moments*, Rahara Enterprises, El Cerrito, vol. 3, 1989.
22 (*a*) M. M. El-Sayed, H. Müller, G. Rheinwald, H. Lang and S. Spange, *J. Phys. Org. Chem.*, 2001, **14**, 247; (*b*) S. Spange, M. M. El-Sayed, H. Müller, G. Rheinwald, H. Lang and W. Poppitz, *Eur. J. Org. Chem.*, 2002, 4159; (*c*) M. M. El-Sayed, H. Müller, G. Rheinwald, H. Lang and S. Spange, *Chem. Mater.*, 2003, **15**, 746.
23 J. F. J. Dippy, R. Goldacre and J. Phillips, *J. Chem. Soc.*, 1948, 2240.
24 G. M. Sheldrick, *Acta Crystallogr., Sect. A*, 1990, **46**, 467.
25 G. M. Sheldrick, *SHELXL-97, Program for Refinement of Crystal Structures*, University of Göttingen, 1997.

